Dynamical Monte Carlo methods for plasma-surface reactions

Vasco Guerra[1]‡ **and Daniil Marinov**[2]

[1]Instituto de Plasmas e Fusão Nuclear, Instituto Superior Técnico, Universidade de Lisboa, 1049-001 Lisboa, Portugal

[2]Laboratoire de Physique des Plasmas, Ecole Polytechnique, F-91128 Palaiseau Cedex, France

Abstract. Different dynamical Monte Carlo algorithms to investigate molecule formation on surfaces are developed, evaluated and compared with the deterministic approach based on reaction-rate equations. These include a null event algorithm, the n-fold way / BKL algorithm and an "hybrid" variant of the latter. NO_2 formation by NO oxidation on Pyrex and O recombination on silica with the formation of O_2 are taken as case studies. It is shown that dynamical Monte Carlo schemes are flexible, simple to implement, describe easily elementary processes that are not straightforward to include in deterministic simulations, can run very efficiently if appropriately chosen and give highly reliable results. Moreover, the present approach provides a relatively simple procedure to describe fully coupled surface and gas phase chemistries. The influence of the grid size on the CPU calculation time and the accuracy of the results, the effect of back diffusion and its inclusion in a deterministic formulation, and the influence of Langmuir-Hinsehlwood recombination involving two physisorbed atoms, are investigated and discussed.

‡ e-mail: vguerra@tecnico.ulisboa.pt

1. Introduction

Surface recombination of atoms and molecule formation on surfaces is a prevalent subject in various areas of plasma science and technology, such as deposition and etching [1–4], volatile organic compound (VOC) oxidation [5–8] or space-vehicle re-entry studies [9–11]. There are countless works dealing with the recombination of a single atomic species to form the parent diatomic molecule, like H_2 [12,13], N_2 [14–16], O_2 [16–18] and Cl_2 [12,19], so that the references given are merely indicative. The heterogeneous formation of heteronuclear and polyatomic molecules, for instance NO [20–25], NO_2 [20–22, 26–29], N_2O [21, 22], O_3 [30, 31] or CO_2 [32, 33], has also been reported in the literature.

This work addresses the general question of modelling molecule formation on silica or Pyrex surfaces. Despite the impressive evolution of atomic scale simulations in recent years [34–40], its application to realistic conditions of molecule formation on silica-based surfaces is still difficult. Moreover, the direct coupling with complex gas-phase chemistry models remains unpractical. In this context, "coarse-gained" mesoscopic models describing the surface in terms of fractional coverages of different adsorption sites, albeit the lack of a true predictive capacity, constitute powerful tools to describe and interpret surface phenomena.

The most common mesoscopic approach to investigate surface kinetics is to adopt a *deterministic* description (DD), where the time-evolution of the adsorbed species and adsorption sites is ruled by a system of reaction-rate differential equations associated with the different elementary processes taken into account [20, 41–47]. A different approach is to use a *stochastic* dynamical Monte Carlo (DMC) scheme [48–53]. DMC methods follow the evolution of one element of the statistical ensemble and simulate the time evolution of the system without dealing with the master equation directly. They are exact, relatively simple to implement regardless the complexity of the kinetics, handle easily probabilities that depend on the local configuration of the system, provide the study of averages, deviations and correlations, and help bridging the gap between molecular dynamics and the macroscopic or less sophisticated mesoscopic approaches. In addition, Monte Carlo methods are particularly suited to study systems where surface diffusion of physisorbed atoms and/or molecules plays an important role. Indeed, while in a Monte Carlo algorithm the rates for surface diffusion are simple to interpret and their general expressions are known, in the reaction-rate deterministic description the calculation of the associated rate coefficients, such as, *e.g.*, those for Langmuir-Hinshelwood recombination involving one adsorbed atom and a diffusing physisorbed atom, always involve additional assumptions and lose some microscopic detail.

The aim of this work is to investigate the validity and efficiency of dynamical Monte Carlo methods in the study of molecule formation on surfaces. Different DMC algorithms are implemented and tested. The first one is a null event method, similar to the ones developed in [48,50]. The second one is close to the formulation of the dynamical Monte Carlo for gas phase chemical reactions proposed in [54, 55] keeping local update and lists [49]. It is indeed a concretization of the general n-fold way algorithm introduced

by Bortz, Kalos and Lebowitz [56], also known as the BKL algorithm. Finally a hybrid scheme is developed, formulated essentially as the BKL algorithm, but with lists only for some specific processes and allowing for a rejection on the choice of the sites where the remaining processes may occur.

Herein we take as case studies NO oxidation on Pyrex pre-treated with an oxygen discharge and O recombination on silica forming O_2. NO oxidation on Pyrex was recently investigated both experimentally [27–29] and theoretically [28, 29], providing a reliable benchmark for the new calculations. The experiments were designed to ensure a good reproducibility and allow an unambiguous interpretation of the results. The measurements were explained considering Eley-Rideal NO oxidation of chemisorbed O atoms and a slow chemisorption of NO_2 molecules, on a surface that exhibits a *distribution of reactivity among the adsorption sites*. This system further provides a relatively simple example where the model describes a *coupled surface and volume kinetics*.

Oxygen recombination on silica has been extensively studied [16, 18, 20, 41, 43–47] and forms another system of interest for the present investigation. It brings new challenges from the modelling point of view, associated with the *role of physisorbed atoms* on the recombination kinetics. On the one hand, the calculation of the relevant reaction rates in a DD becomes more complex and less rigorous. For instance, the comparison of the deterministic and stochastic simulations evince the role of *back diffusion* and impose a correction to the diffusion term in the DD from [45]. On the other hand, the processes involving thermal desorption and surface diffusion introduce additional and much shorter timescales, that expose the DMC algorithms to very demanding computational conditions. These extreme conditions lead us to propose the aforementioned variant of a dynamical Monte Carlo scheme, which is subsequently used to investigate the influence of the encounters between two physisorbed atoms on the atomic recombination probability.

The structure of this paper is as follows. The theoretical formulation and the description of the various dynamical Monte Carlo algorithms are detailed on section 2. The results are presented and discussed in section 3. It contains one subsection devoted to the study of NO_2 formation from NO oxidation, where the base DMC methods are validated, evaluated and compared, and another one dedicated to O-atom recombination on silica, which includes the analysis of the new algorithm and an investigation on the relevance of elementary processes involving two physisorbed atoms. Finally, section 4 summarises the main results and closes the paper.

2. Theoretical formulation

Dynamical Monte Carlo (DMC) methods aim at simulating the *time evolution* of a physical system within a stochastic approach, described analytically by the master

equation

$$\frac{\partial P(\sigma,t)}{\partial t} = \sum_{\sigma'} \left[W(\sigma' \to \sigma) P(\sigma',t) - W(\sigma \to \sigma') P(\sigma,t) \right] \ . \tag{1}$$

Here, $P(\sigma,t)$ is the probability of finding the system in state σ at instant t, σ and σ' are successive states of the system and $W(\sigma \to \sigma')$ is the probability per unit time that the system undergoes a transition from state σ to state σ'.

The master equation describes a memoryless process where the transition to the next state does not depend on the past history of the system and depends exclusively on its current state, *i.e.*, it describes a Markovian process. Hence, although it can be constructed intuitively, it may be derived from more fundamental bases [53]. In what concerns the study of surface kinetics, the Markov chain assumption is valid as long as the simulated events, such as thermal desorption, surface diffusion or recombination, are rare. In particular, they should occur on a much longer timescale than the lattice vibrations, so that both timescales become decoupled [53]. In this case, the memory of which states were previously visited is effectively lost due to the vibrations between two transitions and the kinetics is properly described by the master equation.

Dynamical Monte Carlo algorithms do not solve explicitly the master equation for a given system, but instead numerically simulate the underlaying Markov process. They should establish a correspondence between Monte Carlo time and real time, as to describe both the dynamics and the steady-state properties of the system. The theoretical foundations of DMC methods were carefully detailed in the seminal papers by Daniel Gillespie [54, 55], focused on the simulation of the time evolution of chemical reactions in a spatially homogeneous system. Accordingly, Gillespie's method considers only the concentration of the different species and not their exact locations. The adaptation of the algorithm to surface kinetics and to a description where the local configuration is kept is relatively straightforward and is detailed below.

There are several variants of dynamical Monte Carlo algorithms, which nevertheless share several common features. A very interesting review of their application to surface kinetics was recently published by Herma Cuppen and co-workers [53]. If the location of the particles is to be tracked, any DMC method should generate the answers to the questions "when, what and where." In short, the system may undergo k transition events,

$$\mathcal{E} = \{e_1, e_2, \cdots, e_k\} \ , \tag{2}$$

characterised by transition rates,

$$\mathcal{R} = \{r_1, r_2, \cdots, r_k\} \ , \tag{3}$$

while the number of particles capable of experiencing a given event is divided as

$$\mathcal{N} = \{n_1, n_2, \cdots, n_k\} \ . \tag{4}$$

Upon the successful choice of "what" and "where," time is advanced by selecting an increment τ randomly selected from an exponential distribution with parameter

$$\lambda = \sum_i n_i r_i = \sum_i \lambda_i \ , \tag{5}$$

namely

$$\tau = \frac{1}{\lambda} \ln\left(\frac{1}{r}\right) \ , \tag{6}$$

where r is a random number drawn from the uniform distribution in the unit interval, as initially proposed in [56]. Expression (6) ensures that the dynamical Monte Carlo methods provide an accurate treatment of time, with the desired correspondence between Monte Carlo time and real time [48, 54].

Two different base DMC algorithms were implemented, with one additional variant in one of them. The first one is the *null event* method developed by Kristen Fichthorn and Henry Weinberg [48]. The general formulation is carefully debated and detailed in that paper and the validity of the algorithm is exemplified with the analysis of a very simplified adsoprtion-desorption system. The algorithm was subsequently applied to more complex plasma-surface systems in [50, 52]. The null event method can be described from the sequence: *i)* pick randomly a surface site; *ii)* check which processes may occur at that site, depending on its occupancy; *iii)* use a random number to verify if any process does happen at that site; *iv)* if something does happen, calculate the time increment according to (6); *v)* update the surface, gas phase concentrations and the different reaction rates; *vi)* repeat the procedure until the desired time. The critical step is step *iii)*. To ensure a correct description of the time-evolution of the system and increase efficiency, a hierarchy of transition rates is created, $\mathcal{W} = \{w_1, w_2, \cdots, w_k\}$, where $w_i = r_i / r_{\max}$ and $r_{\max} = \max\{\mathcal{R}\}$. Then, once the site is selected, it is verified which event i make occur and a random number is drawn from the uniform unit interval; the event takes place if $r < w_i$; otherwise there is a null-event and the algorithm goes back to *i)*. Clearly, this method is better suited to systems where the various rates w_i are similar. If the rates significantly differ, then the number of null events becomes important and the efficiency of the algorithm decreases. Since in surface kinetics the rates of elementary processes can span over several orders of magnitude [41], a more appropriate algorithm is most certainly desirable.

The second DMC algorithm is closer to the formulation proposed by D. Gillespie [54, 55], with local update and lists [49]. In this scheme, for each potential event a list is kept with the surface sites where it can possibly occur. In this case the algorithm can be informally described as: *i)* chose the next event type, by drawing a random number according to the appropriate probability density function [54, 55]; *ii)* chose randomly, *from the list of possible sites for this event to happen*, the site where it will take place; *iii)* calculate the time increment according to (6); *iv)* update the surface, gas phase concentrations and the different reaction rates; *v)* repeat the procedure until the desired time. The choice of the event type at step *i)* is made by drawing a uniform random number between 0 and λ [*cf.* (5)] and verifying to which interval $[0, \lambda_1), [\lambda_1, \lambda_1 + \lambda_2), \cdots$ it corresponds. Step *ii)* ensures that there are no null events in this scheme. This formulation corresponds in fact to an implementation of the $n-$fold way / BKL algorithm [56], originally designed to study Ising spin systems.

Finally, a hybrid method is implemented to undertake the study O-atom recombination in silica forming O_2 molecules described in in section 3.2. In this system, it turns our that the fractional coverage of physisorption sites can be very low, in the range $10^{-7} - 10^{-4}$ [45], and a large number of physisorption sites is necessary in order to obtain meaningful simulations. However, at each instant most of these sites will be empty, so that keeping and handling a very large list of empty physisorption sites is unpractical and can be very expensive from the computational point of view. The hybrid algorithm consists in an adaptation of the BKL one just described, but where step *ii*) is modified. One the one hand, lists of sites are kept for all events except physisorption (see section 3.2). For these events step *ii)* is the same as before. On the other hand, if the selected event is physisorption, then the site where it takes place is taken randomly from *all* possible sites. It is then verified *a posteriori* if the selected site is a physisorption site and it is empty – and in this case a physisorption event occurs –, or if this is not the case – and another site is taken randomly from all possible sites, until an empty physisorption site is selected. This scheme is hybrid in the sense that it is essentially the BKL algorithm but there could be a "null event" in the selection of a physisorption site. In practice, due to the low density of chemisorption sites and the low fractional coverage of physisorption sites (see section 3.2), it is very rare that a second attempt is necessary to chose the site where physisorption takes place. Hereafter this algorithm is denoted as BKL*.

It is worth noting that in all the DMC schemes tested it is possible to simulate the time-evolution of both gas phase and surface densities in a coupled way. This is actually done in section 3.1. Moreover, besides providing the time-evolution of the system, the current simulations allow a straightforward calculation of the recombination probabilities simply by counting recombination events, as further detailed in section 3.

3. Results and discussion

This section evaluates the accuracy and performance of the dynamical Monte Carlo algorithms for plasma-surface reactions just described. A comparison with the results from a more traditional deterministic description is also carried out. Two systems are investigated, testing and focusing on different aspects of surface kinetics: Eley-Rideal NO recombination with chemisorbed O-atoms to form NO_2 (section 3.1) and both Eley-Rideal and Langmuir-Hinshelwood O recombination to form O_2 (section 3.2). The former system involves chemisorption and recombination on a surface with a *distribution of reactivity* among different adsorption sites, as well as a *coupling between gas phase concentrations and surface kinetics* that results in *time-dependent rates* for the elementary processes taken into account. In turn, the latter system is interesting to study *physisorption* and elementary *processes involving physisorbed atoms*, which induce rates that can *span over nine orders of magnitude*, point out the need to account for *back diffusion* in deterministic models, and allows to investigate the role of *recombination of two physisorbed atoms* (usually neglected in DD studies).

3.1. NO oxidation on pre-treated Pyrex with NO_2 formation

The first system under analysis is the formation of NO_2 molecules on a Pyrex tube of inner radius 1 cm, as a result of NO oxidation by previously adsorbed O atoms on the wall. The experiments and the deterministic model were described in detail in [27–29]. In summary, an oxygen discharge is used to graft O atoms on the wall; the discharge tube is then pumped for about 10 minutes to remove gas phase species and let the temperature cool down to room temperature; finally, a controlled amount of NO diluted in argon is introduced, corresponding to pressures between 0.1 and 4 Torr, and the time-dependent gas phase NO and NO_2 concentrations are measured using a diode laser spectrometer.

As discussed in [28, 29], the surface exhibits a distribution of reactivity among the adsorption sites. A very good simulation of the experimental results was achieved in [29], by considering 7 types of chemisorption sites, with different activation energies for recombination, together with a relatively simple kinetics described by the following reactions:

(i) Eley-Rideal NO oxidation,

$$NO + O_S(i) \xrightarrow{r_1(i)} NO_2 + S_V(i) \ ,$$

where $O_S(i)$ and $S_V(i)$ represent an adsorbed oxygen atom on a chemisorption site of type i and a vacant chemisorption site of type i, respectively;

(ii) slow NO_2 chemisorption on vacant sites,

$$NO_2 + S_V(i) \xrightarrow{r_2(i)} (NO_2)_S(i) \ .$$

The corresponding rates are given and discussed in [29],

$$r_1(i) = k_1^{0\prime}(i)\varphi_i \frac{\phi_{NO}}{[S_i]} \exp\left(-\frac{E_R(i)}{kT_W}\right) \ \text{site}^{-1}\text{s}^{-1} \tag{7}$$

and

$$r_2(i) = k_2^{0\prime}(i)\varphi_i \frac{\phi_{NO_2}}{[S_i]} \ \text{site}^{-1}\text{s}^{-1} \ . \tag{8}$$

Here, the preexponential factor $k_1^{0\prime}(i)$ is set to 1, φ_i is the fraction of the surface covered with chemisorption sites of type i, $[\text{S}_i]$ is the surface density of chemisorption sites of type i, k is the Boltzmann constant, $T_W = 300$ K is the gas temperature very close to the wall, $E_R(i)$ is the activation energy for recombination at sites i, and

$$\phi_{NO} = \frac{1}{4}\langle v_{NO}\rangle [NO] \tag{9}$$

is the flow of NO molecules to the wall, [NO] denoting the gas phase concentration of NO molecules, and

$$\langle v_{NO}\rangle = \sqrt{\frac{8kT_g}{\pi M_{NO}}} \tag{10}$$

the thermal speed of NO molecules, where $T_g = 300$ K is the gas temperature and M_{NO} the mass of the NO molecules, and a similar expression is used for ϕ_{NO_2}. Finally,

the slow NO_2 chemisorption is modelled using a small elementary sticking probability, $k_2^{0\prime}(i) = 5 \times 10^{-8}$, the same for all i. According to these definitions,

$$\varphi_i = \varphi\, \delta_i \ , \tag{11}$$

where δ_i is the fraction of chemisorption sites that have type i. The values for δ_i and for the activation energies $E_R(i)$ are given in [29]:

$$\delta_i = \{0.01, 0.02, 0.03, 0.06, 0.14, 0.25, 0.49\} \ , \tag{12}$$

$$E_R(i) = \{16, 21, 24, 29, 33, 39, 41\} \text{ kJ/mol.} \tag{13}$$

The total density of chemisorption sites was determined from experiment, $[S] \simeq 2.5 \times 10^{14}$ cm^{-2} [16]. Hence, considering a unit roughness factor, the fraction of the surface covered with chemisorption sites is $\varphi \simeq 2 \times 10^{-1}$ [45]. The fractional coverage of the different adsorption sites is defined as

$$\theta_M(i) = \frac{[M_S(i)]}{[S_i]} \ . \tag{14}$$

When a deterministic description is adopted, the system of equations to be solved can be written in the form

$$\frac{d\theta_O(i)}{dt} = -\, r_1(i)\theta_O(i) \tag{15}$$

$$\frac{d\theta_{NO_2}(i)}{dt} = [1 - \theta_O(i) - \theta_{NO_2}(i)]\, r_2(i) \tag{16}$$

$$\frac{d[NO]}{dt} = -\, \frac{2}{R} \left(\sum_{i=1}^{7} \theta_O(i)[S_i] r_1(i) \right) \tag{17}$$

$$\frac{d[NO_2]}{dt} = \frac{2}{R} \sum_{i=1}^{7} \{\theta_O(i) r_1(i) - [1 - \theta_O(i) - \theta_{NO_2}(i)]\, r_2(i)\}\, [S_i] \ . \tag{18}$$

This system was solved in [29] using an implicit Runge-Kutta method. Taking into account the excellent agreement between the deterministic model calculations and the experimental results reported in [27–29], the DD calculations are used as a benchmark for the present study. Notice as well that this system does not presuppose reactions with physisorbed atoms, so that the DD does not involve any additional assumptions as compared to the ones required to develop a DMC simulation.

To run a particular simulation, the total number of chemisorption sites actually followed in the simulation, $[\tilde{S}]$, has to be defined. The calculation of the fractional coverages (14) from the simulation results is then immediate, from the fractions of simulation sites that are occupied at each instant. The conversation from "simulation particles" or "simulation sites" to real surface and volume densities in equations (17) and (18) is also straightforward, since both $[S]$ and $[\tilde{S}]$ are given. Denoting with a $\tilde{}$ simulation particles and simulation sites, an effective simulation length L can be defined from the relation

$$[S] = \frac{\tilde{S}}{2\pi R L} \ . \tag{19}$$

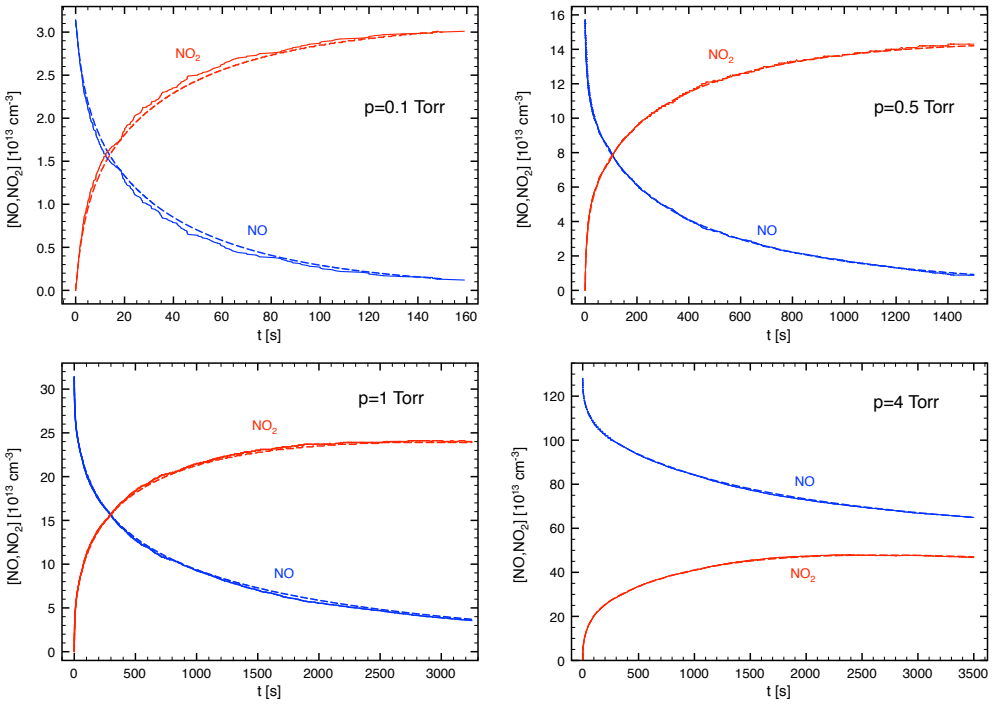

Figure 1. Time-evolution of NO and NO_2 calculated from the DMC BKL algorithm with $[\tilde{S}] = 7500$ (—) and the DD (– –), for four values of pressure.

Then, for the gas phase concentrations of species M=NO, NO_2,

$$[M] = \frac{\tilde{M}}{\pi R^2 L} \ , \tag{20}$$

so that the conversion from simulation particles to actual gas phase densities is given by

$$[\tilde{M}] = [M]\frac{[\tilde{S}]}{[S]}\frac{R}{2} \ , \tag{21}$$

where the factor $R/2$ is just the Volume/Surface ratio.

To validate the DMC algorithms, figure 1 shows the calculated time-evolution of NO and NO_2 gas phase concentrations for four values of pressure, in the range 0.1–4 Torr, obtained in a single run of the BKL algorithm with $[\tilde{S}] = 7500$ (full curves). The results of the deterministic description corresponding to the Runge-Kutta solution to the reaction-rate model, previously obtained in [29], are also represented (dashed lines). As it can be seen, the curves are practically indistinguishable, which confirms that the dynamical Monte Carlo method furnishes a consistent simulation of the system for all conditions and describes well characteristic evolution timescales that vary significantly.

It has been verified that the two DMC algorithms (null event and BKL) lead to very similar results, as expected, and that figure 1 is reproduced using the null event

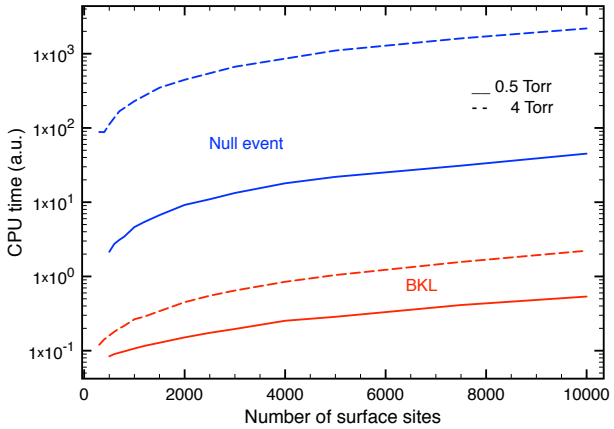

Figure 2. Comparison of the CPU time used by the BKL and the null event DMC algorithms as a function of the number of surface sites, for $p = 0.5$ (—) and 4 (– –) Torr.

algorithm. Therefore, in principle, the choice of one or the other has to be made in terms of simplicity of use and computational efficiency. The former criterion, however, does not play a significant role in the decision, as both schemes are relatively easy to implement. The computation time is thus the decisive criterion. Figure 2 shows the average CPU time used by each of the methods, as a function of the number of surface sites $[\tilde{S}]$ used in the simulation, for two values of pressure. It is immediate to verify that the BKL algorithm is much more efficient than the null event method, in accordance with the results from [49]. The CPU calculation times are between one and three orders of magnitude shorter for the BKL algorithm. The better performance of this method is not very surprising, since the rates in (7) and (8) differ at least by four orders of magnitude.

Our analysis of DMC simulations for surface kinetics continues with the study of the influence of the grid size and of averaging on the accuracy of the results. Since the BKL and null event algorithms give similar results and the former is computationally more efficient, all calculations presented in the remaining of the current subsection are made with this algorithm.

A detailed inspection of figure 2 reveals that, for this system, the CPU computation time scales linearly with the number of surface sites used. It is therefore important to quantify the tradeoff between the gain in computational time resulting from considering a smaller number of surface sites in the simulation and the loss of quality of the statistics. An illustration of the latter effect is shown in figure 3, where two values of $[\tilde{S}]$ are used for a single run of the $p = 1$ Torr case, namely 500 and 7500 sites. The general time-evolution of the gas phase concentrations of NO and NO_2 molecules is well described in both cases. However, larger fluctuations around the values obtained from

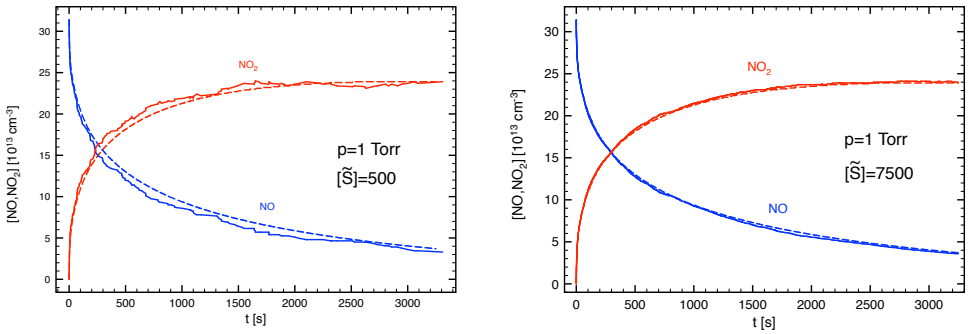

Figure 3. Time-evolution of NO and NO_2 calculated for $p = 1$ Torr from: the DMC BKL algorithm for two values for the total number of surface sites $[\tilde{S}]$ (—); the DD (– –).

the deterministic description are evident when only 500 surface sites are used. These fluctuations do not correspond to any physical effect and are merely a consequence of the insufficient size used for the description of the surface. Note that the sites with the three highest reactivities correspond only to 1%, 2% and 3% of the total number surface sites [*cf.* expression (12)], so that when $[\tilde{S}] = 500$ there are only 5, 10 and 15 sites of these types in the simulation. The calculation made with 7500 sites provides results barely distinguishable from the expected ones.

The qualitative indications from figure 3 can be quantified, for instance, by introducing an absolute error defined as the average of

$$\Delta = \sqrt{\sum_{i=1}^{N} \left([NO]_{DMC}(i) - [NO]_{DD}(i) \right)^2} \tag{22}$$

over 50 realisations of the system. Here, the concentrations $[NO]_{DMC}(i)$ and $[NO]_{DD}(i)$ are single run DMC and the DD values calculated at $N = 100$ different time instants. A similar definition is used to obtain the absolute error associated with the calculated time-evolution of NO_2 molecules. Figure 4 shows these two absolute errors, for the cases $p = 0.5$ and $p = 4$ Torr. For completeness, it also shows the average CPU time used in the simulations, confirming its linear growth with $[\tilde{S}]$. The error decreases about a factor of 3-4 when the number of surface sites in the simulation increases from 500 to 10000, with a strong reduction while $[\tilde{S}]$ remains below 1500-2000 sites. However, there is a tendency for a certain saturation, in the sense that an increase of $[\tilde{S}]$ beyond a certain limit continues to improve the accuracy of the results, but at a much smaller rate.

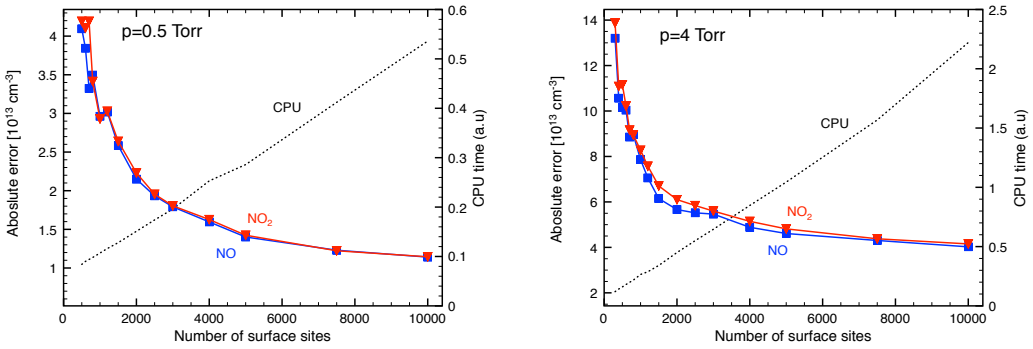

Figure 4. Absolute error associated with NO (■) and NO_2 (▼) and CPU time as a function of the number of surface sites, for $p = 0.5$ and 4 Torr.

Another possibility to reduce the statistical fluctuations around the average values, as an alternative to the increase in the number of surface sites considered in a single simulation, is to actually average the results over several realisations of the system. The latter procedure is formally more appealing, as it corresponds to follow different points of the statistical ensemble. As a matter of fact, good practices suggest to perform averages even if the number of surface sites is large enough to ensure smooth dependencies of the different quantities on a single run. In addition, averaging over several simulations can be interesting from the computational point of view, as different runs can be launched on different computer cores. As such, this procedure may bring a significant gain in the (real) time it takes to obtain one result, albeit may be not in the used cpu time.

In order to qualitatively evaluate the effect of the averaging procedure, the results obtained on a single run and averaging over three and five runs are represented in figure 5, for $p = 0.5$ Torr and considering a relatively small number of surface sites, $[\tilde{S}] = 800$. The dashed lines are the concentrations calculated form the reaction-rate deterministic description. The influence and efficacy of averaging is clearly visible from the figure, confirming it does reduce the importance of fluctuations, as it should be expected.

The quantitative analysis of the effectiveness of both strategies to reduce fluctuations is presented in figure 6, where the absolute error defined above (average value of Δ over 50 runs) is plotted against the total CPU time consumed, for two values of pressure and using each of the methods. As it can be verified, the CPU time required to obtain a particular accuracy is quite insensitive to the procedure used. This confirms that it may be advantageous to use smaller simulations and perform averages, as compared to increasing the number of surface sites, in particular for systems which

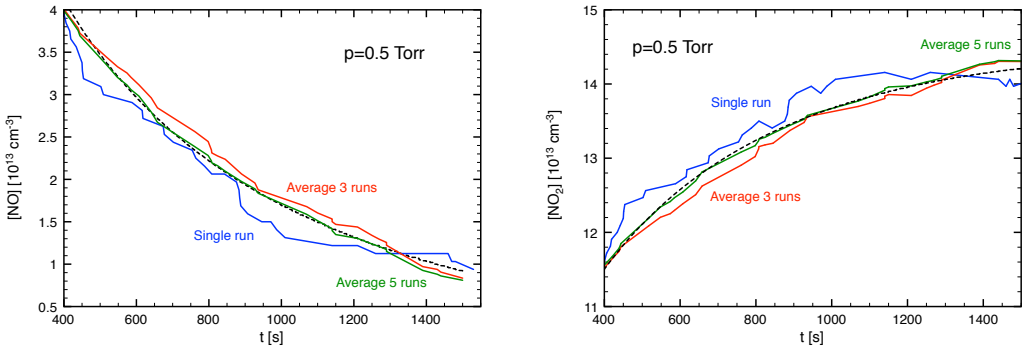

Figure 5. Time-evolution of NO and NO_2 calculated for $p = 0.5$ Torr from: the DMC BKL algorithm and $[\tilde{S}] = 800$ (—), on a single run, and averaging over 3 and 5 runs; the DD (– –).

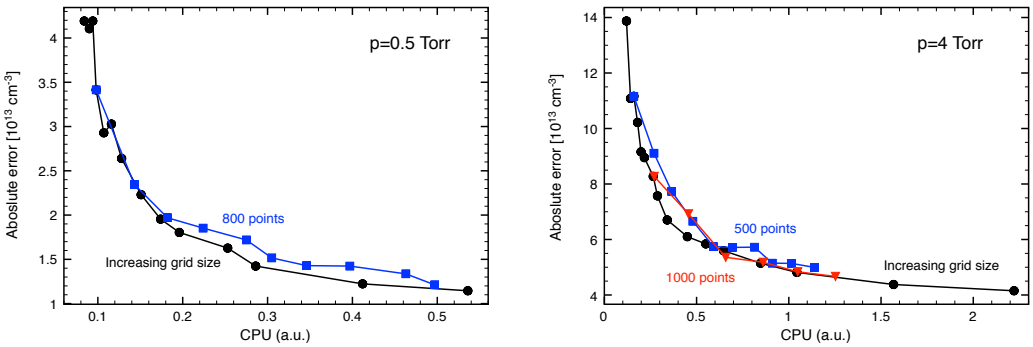

Figure 6. Absolute error associated with NO as a function of the used CPU time for $p = 0.5$ and 4 Torr, by increasing the number of surface sites $[\tilde{S}]$ (•), or the number of runs to average as follows: $[\tilde{S}] = 800$ and $p = 0.5$ Torr (■) ; $[\tilde{S}] = 500$ and $p = 4$ Torr (■) ; $[\tilde{S}] = 1000$ and $p = 4$ Torr (▼)

demand very long simulations and if it is possible to launch several runs in parallel.

3.2. O recombination in O_2 on silica

Heterogeneous oxygen atomic recombination on silica or on Pyrex was extensively studied, both experimentally [42, 44, 46, 47, 57, 58] and with mesoscopic deterministic models [20, 41–47]. The set of elementary processes taken into account in deterministic models often comprises physisorption, thermal desorption from physisorption sites, chemisorption, surface diffusion of physisorbed atoms, and both Eley-Rideal (E-R) and Langmuir-Hinshewood (L-H) recombination [17,20,41,44,45], which can be represented, respectively, as

$$O + F_V \xrightarrow{r_1} O_F \tag{R1}$$

$$O_F \xrightarrow{r_2} O + F_V \tag{R2}$$

$$O + S_V \xrightarrow{r_3} O_S \tag{R3}$$

$$O + O_S \xrightarrow{r_4} O_2 + S_V \tag{R4}$$

$$O_S + S_V \xrightarrow{r_5} S_V + O_S \tag{R5}$$

$$O_F + O_S \xrightarrow{r_6} O_2 + S_V + F_V \tag{R6}$$

Here, O and O_2 are gas phase oxygen atoms and molecules, O_F and O_S are physisorbed and chemisorbed oxygen atoms, while F_V and S_V are vacant physisorption and chemisorption sites.

O-atom recombination forming O_2 as described by reactions (R1–R6) constitutes a very interesting system for the purposes of the present investigation. Firstly, it brings additional challenges associated with the surface processes involving physisorbed oxygen atoms. These processes induce a much larger variation on the characteristic time-scales of the different mechanisms, allowing to test the dynamical Monte Carlo algorithms in rather extreme conditions. Secondly, DMC has a simple and straightforward treatment of surface diffusion mechanisms and the simulations can be used to validate the approximations made in the deterministic description. Finally, it is a system of great practical interest *per se* and that can serve as the basis for further research, for instance the study of the formation of more complex molecules on the surface, like O_3 and CO_2, or the influence of a distribution of reactivity among the chemisorption sites as described in subsection 3.1 on the O-atom recombination probability. Such generalisations go beyond the scope of this paper and are planned for the near future.

The expressions for the different processes (R1–R6) were reviewed and discussed in [45]. The physisorption and chemisorption rates are given by equations similar to (8),

$$r_1 = \frac{k_1^0}{[F]+[S]}\phi_O \quad \text{site}^{-1}\text{s}^{-1} \tag{23}$$

$$r_3 = \frac{k_3^0}{[F]+[S]}\phi_O \quad \text{site}^{-1}\text{s}^{-1} \tag{24}$$

where k_1^0 and k_3^0 are elementary sticking probabilities on physisorption and chemisorption sites, ϕ_O is the flow of oxygen atoms to the surface given as in (9), and $[F]$ and $[S]$ are

the surface densities of physisorption and chemisorption sites. The thermal desorption rate is given by

$$r_2 = \nu_d \exp\left(-\frac{E_d}{kT_W}\right) \quad \text{site}^{-1}\text{s}^{-1} \ , \tag{25}$$

where ν_d is a frequency factor that for low adsorbate concentrations can be associated with the vibration of physisorbed atoms on the direction perpendicular to the surface [59, 60], and E_d is an energy barrier for desorption. The rate of Eley-Rideal recombination is given similarly to (7),

$$r_4 = P_R r_3 \quad \text{site}^{-1}\text{s}^{-1} \tag{26}$$

where P_R is the elementary recombination probability,

$$P_R = k_4^0 \exp\left(-\frac{E_R}{kT_W}\right) \tag{27}$$

and E_R is the activation energy for recombination. The rates for processes (R5) and (R6) involving the diffusion of physisorbed atoms are given in [45]. They are calculated assuming that the average time between hops from one physisorption site to a neighbouring site due to diffusion, τ_D, is given by

$$\tau_D^{-1} = \nu_D \exp\left(-\frac{E_D}{kT_W}\right) \ , \tag{28}$$

where ν_D can be associated with a frequency of vibration parallel to the surface and E_D is the energy barrier for diffusion, typically $E_D \simeq 0.5 E_d$ [41]. Expression (28) is all that is necessary to simulate the mechanisms (R5) and (R6) within a dynamic Monte Carlo approach. On the deterministic description some additional assumptions have to be made [41, 45]. For most cases of interest here the expressions given in [45] can be approximated by

$$r_5 \simeq \frac{\nu_D}{\nu_d} \exp\left(\frac{E_d - E_D}{kT_W}\right) r_2 \quad \text{site}^{-1}\text{s}^{-1} \tag{29}$$

and

$$r_6 \simeq P_R r_5 \quad \text{site}^{-1}\text{s}^{-1} \tag{30}$$

Notice that the rate r_5 should be corrected to account for *back diffusion*, with a reduction by a factor of 3/4 in case of a square grid. This effect expresses the fact that the diffusing particles can revisit adsorption sites multiple times when they undergo a random walk on the surface [53] and is further discussed and illustrated below [*cf.* figure 10]

The values of the different surface parameters considered in the current simulations are summarised in table 1. They correspond to typical values in these studies and lead to calculations in very good agreement with a large set of experimental data [*cf.* figure 7]. Nevertheless, other values have been used by different authors, as the examples below typify.

- The density of physisorption sites is sometimes assumed to be larger, $[F] \sim 10^{16}$ cm^{-2} [33, 45–47].

- The fraction of the surface occupied by chemisorption sites, $\varphi = [S]/([F] + [S])$, was assumed by different authors to be 1×10^{-3} [46], 2×10^{-3} [45], 5×10^{-2} [33], or 6×10^{-2} [61], and experimentally estimated in [16] with a larger value, 2×10^{-1}. The dispersion of values is common in surface studies and is likely to be related to the very nature of the chemisorption sites on silica surfaces, with the restructure and modification of the surface induced by plasma exposition and the possible participation of oxygen atoms from the material in the recombination process [16].
- The activation energy for desorption (30 kJ/mol) is very close to the values used in [20, 45] (33.3 kJ/mol) and in [46, 47] (31.6 kJ/mol), albeit smaller than the 51 kJ/mol from [41].
- Reported values for the activation energy for recombination include 15.8 kJ/mol [46, 47] and 17 kJ/mol [41], quite similar to the one used here (17.5 kJ/ml), as well as the somewhat larger 25 kJ/mol [33] and 25.5 kJ/mol [45]. Dmitry Lopaev and co-workers [46] give an interesting argument that E_R should be similar to E_D, by noting that even in E-R recombination the incoming gas phase atom has first to be physisorbed nearby the chemisorbed atom and then has to surmount the activation energy for diffusion to arrive at the chemisorbed atom. The argument is certainly disputable, but it is worth noting that indeed $E_R \simeq E_D$ in the present calculations.
- The frequency factor ν_d is carefully discussed in [59]. In principle it depends on the gas temperature close to the wall, T_W [11, 59]. Transition-state-theory predicts a linear dependence with T_W, $\nu_d = kT_W/h \simeq 6 \times 10^{12} \left(\frac{T_W[K]}{300}\right)$ s^{-1} if the activated complex and the adsorbed species have the same partition function [60]. This justifies the value $\sim 10^{13}$ s^{-1} frequently assumed, as in [17, 46]. However, if the transition state complex is less strongly bound to the surface, *i.e.*, it represents a molecule "ready" for desorption, it may have higher degrees of freedom and the frequency factor can increase up to 10^{16} s^{-1} [60]. The formulation by Ibach and co-workers [59] also suggests a frequency factor more of the order of 10^{15} s^{-1} than 10^{13} s^{-1}.

Except otherwise noticed the results presented in this subsection are obtained for wall temperature $T_W = 300$ K, gas temperature $T_g = 500$ K and gas phase atomic concentration $[O] = 10^{15}$ cm^{-3}.

At steady-state, the recombination probability of atomic oxygen calculated according to the heterogeneous kinetic scheme (R1)–(R6) is given by [45]

$$\gamma_O = \frac{2\theta_S(r_4 + \theta_F r_6)}{\phi_O}[S] \equiv \gamma_{ER} + \gamma_{LH} \ , \tag{31}$$

where the individual contributions from E-R and L-H recombination are clearly identified, θ_S and θ_O are the fractional coverages of physisorption and chemisorption sites, respectively, and the roughness factor defined as the ratio of the real surface area to the geometric area was assumed to be 1 [20, 45]. The result is represented in figure 7, as a function of the wall temperature, for the surface parameters in table 1. Despite the dispersion of the high temperature data, there is generally a quite

k_1^0	1
k_3^0	1
k_4^0	1
$[F]$	1.5×10^{15} cm^{-2}
$[S]$	3×10^{13} cm^{-2}
φ	2×10^{-2}
ν_d	10^{15} s^{-1}
ν_D	10^{13} s^{-1}
E_d	30 kJ/mol
E_D	$E_d/2 = 15$ kJ/mol
E_R	17.5 kJ/mol

Table 1. Surface parameters used in the simulations

good agreement between the model calculations and both the experimental results shown and the calculations by other authors (themselves based on comparisons with experimental data). In particular, the region around 300–400 K is very well described, and at $T_W = 300$ K the calculations coincide with the recent measurement from [31]. The global behaviour of γ_O with T_W is the outcome of the competition between between the E-R and L-H recombination mechanisms. For $T_W \lesssim 380$ K Langmuir-Hinshelwood recombination is dominant, in agreement with the conclusions from [20].

For the dynamical Monte Carlo simulations in this work the surface is represented as a square lattice and a diffusing atom may hop in one of fourth equally likely directions. The hopping of diffusing physisobed atoms is directly described by (28). The corresponding event and rate are included in the sets $\mathcal{E}$ and $\mathcal{R}$ defined by (2) and (3) and the rate is used in the calculation of the time increment (5). The macroscopic rates r_5 (29) and r_6 (30) are never used. *A priori* the list of sites where there are physisorbed atoms in condition to diffuse is the same as the one identifying the sites where a physisorbed atom can desorb, so there is no need to consider a separate list. In fact, from the implementation point of view it is possible to consider a single event "diffusion or desorption" with a total rate $r_2 + \tau_D^{-1}$ which, if chosen, can then be deconvoluted in the two sub-events. The average rates of the various processes considered in the DMC simulations are given in table 2, for the base conditions of this study (surface parameters of table 1, $T_g = 500$ K, $T_w = 300$ K and $[O] = 10^{15}$ cm^{-3}).

For the system under investigation, no list should be considered to store the surface sites holding empty physisorption sites. The reason is that the current simulations require a large grid of sites to represent te surface, as a result of the low fractional coverage of physisoroption sites, in the range $10^{-7} - 10^{-4}$ [45] (*cf.* as well figure 9). Keeping track and handling a large list of empty physisorption sites is extremely expensive from the computational point of view. The solution is to use the BKL* "hybrid" algorithm described in section 2, that uses lists for all events except

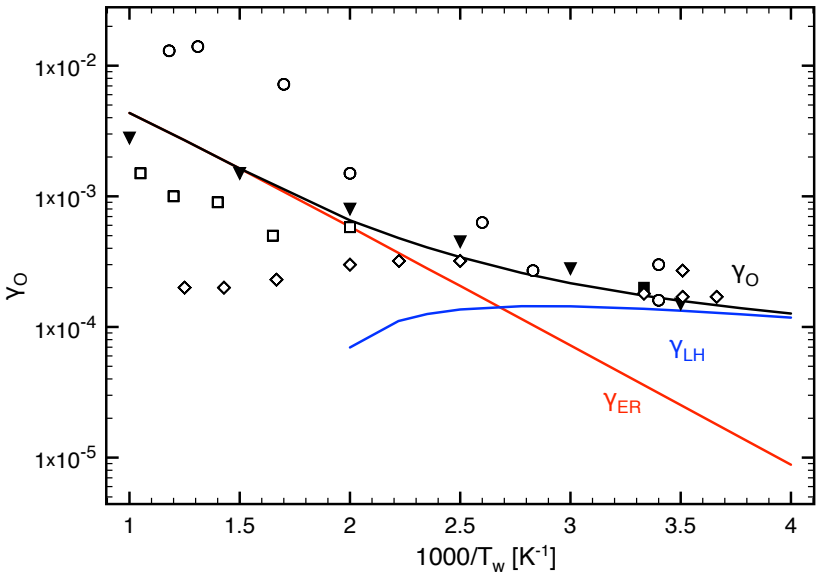

Figure 7. O-atom recombination probability as a function of the wall temperature: measured in [57] (○); measured in [41] (◇); calculated in [42] (□); calculated in [20] (▼); measured in [31] (■); and calculated according to the surface kinetic scheme (R1–R6) (full curves) – (—) Langmuir-Hinshelwood recombination, (—) Eley-Rideal recombination, (—) total.

Process	Average rate ($\text{site}^{-1}\text{s}^{-1}$)
physisorption	1.3×10^4
desorption	6.0×10^9
chemisorption	1.3×10^4
E-R recombination	1.2×10^1
diffusion	2.4×10^{10}

Table 2. Average rates of the different processes considered in the base DMC simulations.

physisorption.

There are a couple of additional details to handle in a DMC simulation. The first one is to decide what happens with a physisorbed atom that reaches an occupied chemisorption site and does not recombine. One possibility would be to assume that the atom would remain physisorbed on the top of the chemisorbed one; on subsequent times it could then diffuse or thermally desorb, as any other physisorbed atom, or attempt recombination with the chemisorbed atom. One other possibility would be to leave it physisorbed in a randomly chosen neighbouring physisorption site. Here, for simplicity,

it is assumed that the physisorbed atom goes back to its original position. Despite the conceptual differences between these scenarios, the results are pretty much independent of the hypothesis made.

The second new question is the fate of the encounters between two physisorbed atoms. As the fractional coverage of physisorbed atoms is usually low [20, 41, 45], these encounters are often neglected in the DD. However, while performing a DMC simulation it will most certainly happen that a diffusing physisorbed atom will hop into an occupied physisorption site. Moreover, according to [46, 47] the recombination of two physisorbed atoms can be the dominant recombination process in DC discharges at intermediate pressures, $p = 10 - 50$ Torr, so it is pertinent to analyse this mechanism in some detail. Reaction (R6) can be re-written as

$$O_F + O_S \xrightarrow{r_{6a}} O_2 + S_V + F_V \tag{R6a}$$

$$O_F + O_F \xrightarrow{r_{6b}} O_2 + F_V + F_V \tag{R6b}$$

The possible influence of this type of encounters was briefly discussed in [50]. Here, it is assumed that when two physisorbed atoms meet they recombine with probability 1 [*i.e.*, pre-exponential factor 1 and activation energy 0 in an expression similar to (27)]. This assumption is justified since the physisorbed atoms are weakly bound to the surface and recombination should be relatively easy, with the surface playing the role of a third body. The same hypothesis was used in [62] for the case of hydrogen recombination on grains in the interstellar medium, where it is considered that H_2 is formed with probability one, although it can remain for a while on the surface as a physisorbed molecule, due to the very low temperatures (5–25 K) considered in that study. For higher temperatures, however, physisorbed molecules formed in recombination are expected to desorb very quickly and they can be presumed to go back to the gas phase upon recombination.

The inclusion of mechanism (R6b) leads to a new term in the recombination probability (31), as defined in a DD. From the gas phase loss term at the wall and the definition of γ_O [45],

$$\begin{aligned}\left(\frac{d[O]}{dt}\right)_W &= -\frac{2}{R}([F_V]r_1 - [O_f]r_2 + [S_v]r_3 + [O_S]r_4) \\ &\equiv -\frac{\langle v_O\rangle}{2R}\gamma_O[O]\end{aligned} \tag{32}$$

In steady-state, it is easy to derive

$$\gamma_O = \gamma_{ER} + \gamma_{LH}^S + \gamma_{LH}^F \ , \tag{33}$$

where

$$\gamma_{ER} = \frac{2\theta_S r_4}{\phi_O}[S] \ , \tag{34}$$

$$\gamma_{LH}^S = \frac{2\theta_F\theta_S r_{6a}}{\phi_O}[S] \ , \tag{35}$$

$$\gamma_{LH}^F = \frac{2\theta_F\theta_F r_{6b}}{\phi_O}[F] \ , \tag{36}$$

$$\tag{37}$$

are the contributions of E-R recombination (R4), L-H recombination according to (R6a) and L-H recombination according to (R6b), respectively. The calculation of the recombination probability γ_O and the identification of the relative importance of the different mechanisms is straightforward in the DMC simulations. Indeed, it is enough to count the number of recombination events of each type i, NRec_i, during a physical time interval Δt where the system has reached "steady-state." The corresponding recombination probability is then given by

$$\gamma_i = \frac{2\mathrm{NRec}_i}{\Delta t} \frac{[S]+[F]}{[\tilde{S}]+[\tilde{F}]} \frac{1}{\phi_O} \,, \tag{38}$$

$[\tilde{S}]+[\tilde{F}]$ denoting the total number of sites actually considered in the numeric simulation. If the simulation is long enough so that the influence of the transient state is negligible, Δt can simply be taken as the full physical time considered and all recombination events can be counted.

The recombination probabilities calculated both from the DD (full lines) and the DMC (points with dotted lines) simulations are shown in figure 8, for wall temperatures between 250 K and 400 K and two different values of the gas phase oxygen atomic concentration, $[O] = 10^{15}$ cm^{-3} and 5×10^{15} cm^{-3}. This figure confirms the power of DMC simulations and allows to evaluate the importance of the recombination mechanism (R6b) involving two physisorbed atoms, not accounted for in the DD calculations. It can be verified that DMC and the DD give very similar results when recombination (R6b) is negligible. Furthermore, this process can become important for low wall temperatures and/or high flows of atoms to the surface. The underlaying reason is that these conditions impose a higher fractional coverage of the physisorption sites, θ_F, as shown in figure 9, so that encounters between two physisorbed atoms become more likely. This conclusion is in line with the inferences from [46, 47] for DC discharges at intermediate pressures stated above. Notwithstanding, in these conditions the fractional coverage θ_F is not affected by the inclusion of process (R6b).

The comparison of the DMC and DD results can be further appreciated by inspection of figure 10, displaying the time evolution of the fractional coverages of physisorbed and chemisorbed atoms for the base calculations, using a 5750×5750 grid. The deterministic calculations are performed including and excluding the 3/4 correction on the rate r_5 to account for *back diffusion*, while DMC results are shown for a single run and an average over three runs. There is a very good correspondence between the DMC and DD calculations. The influence of back diffusion in the DD results is evident during the transient period. Interestingly enough, the steady-state values are not affected by this correction. Finally, the outcome of the averaging procedure delineated in subsection 3.1 as a procedure to reduce statistical fluctuations is also clearly visible.

To bring this section to an end, it is worth making a quantitative judgement on the efficiency of the different DMC algorithms for the simulation of the oxygen recombination system. Both the null-event and the standard BKL algorithm are much longer to run than the hybrid BKL* scheme proposed here. The computational burden makes a thorough comparison unrealistic, but some indications can be given anyway.

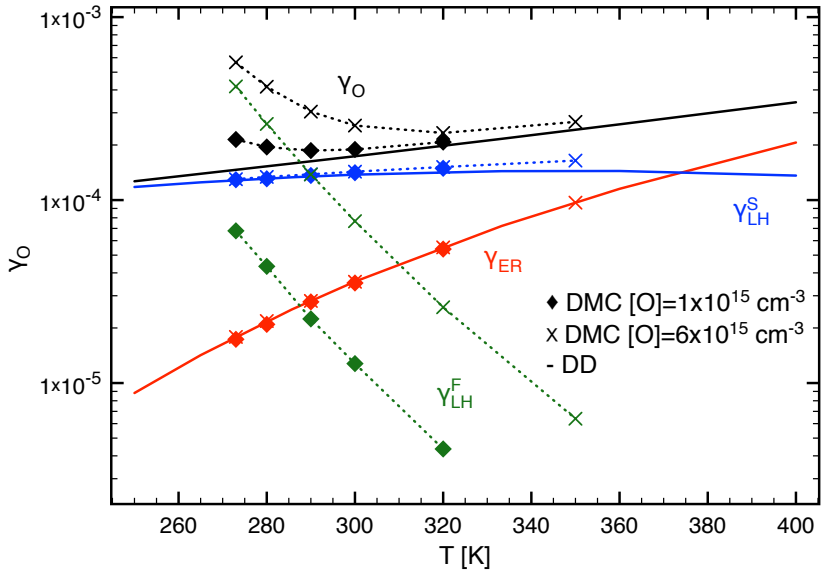

Figure 8. Oxygen recombination probability as a function of the wall temperature calculated from the DMC with $[O] = 10^{15}$ cm^{-3} ($\cdot\blacklozenge\cdot$) and $[O] = 5 \times 10^{15}$ cm^{-3} ($\cdot \times \cdot$), and from the DD (—) (the two cases are indistinguishable): γ_{ER} (red); γ^S_{LH} (blue); γ^F_{LH} (green); total (black).

Grid size	1000×1000	1500×1500	2000×2000
BKL	1878	9316	30898
BKL*	1	3	9

Table 3. CPU time (a.u.) for the BKL and BKL* algorithms as a function of the grid size.

The efficiency of the BKL and BKL* algorithms was tested as a function of the grid size, for a final simulation time of 10^{-4} s. The results obtained on a single run are given in table 3. As discussed in section 2, in the hybrid scheme "null events" to chose an empty physisorption site practically never happen and the BKL* algorithm is by far faster, by a factor of about $(2-3) \times 10^3$. Other tests performed confirm similar gains in speed, between 2 and 4 orders of magnitude.

Finally, the performance of null event and the BKL* DMC algorithms was compared on a 2000×2000 grid, when the desorption energy E_d varies between 30 kJ/mol and 51 kJ/mol and the diffusion frequency ν_D was reduced from 10^{13} s^{-1} to 10^{12} s^{-1}. All other parameters were kept as in table 1. The reduction in ν_D is simply an artefact to speed up the calculations and easy the comparison of both methods. As for the variation with E_d, when the desorption energy is increased the the null even algorithm is expected to

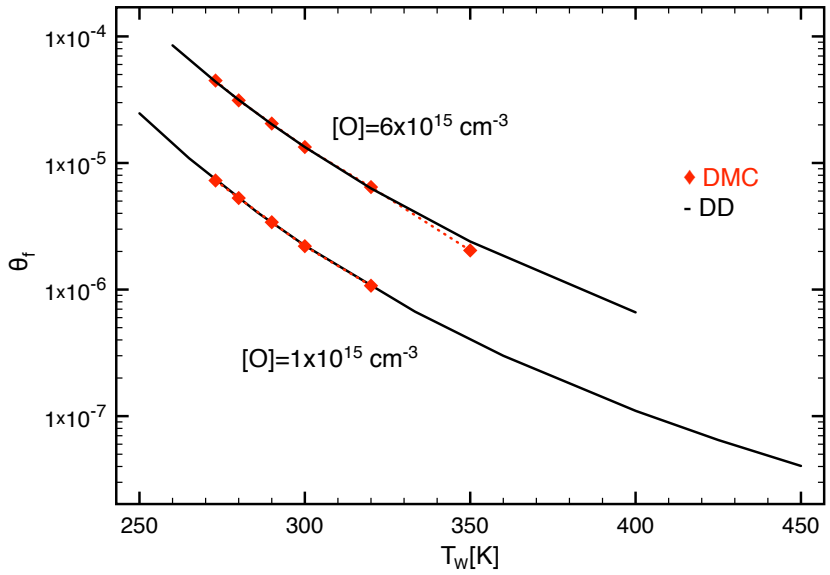

Figure 9. Fractional coverage of physisorption sites as a function of the wall temperature calculated from the DMC (·♦·) and the DD (—), for $[O] = 10^{15}$ cm^{-3} and $[O] = 5 \times 10^{15}$ cm^{-3}

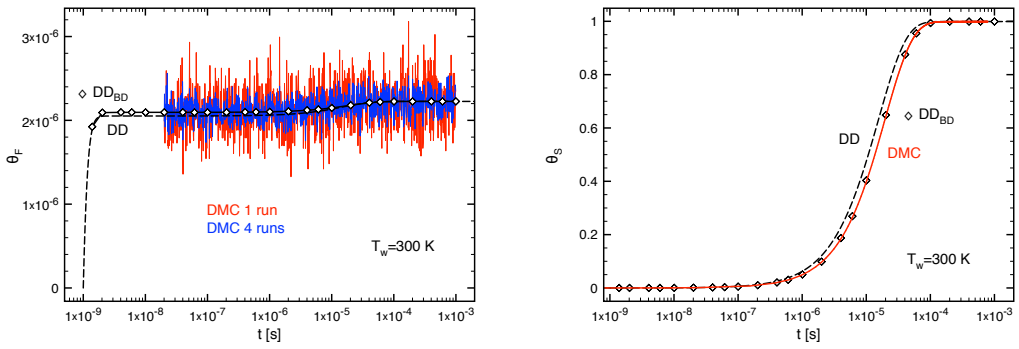

Figure 10. Time-evolution of the fractional coverages of physisorbed (θ_F) and chemisorbed (θ_S) sites on a 5750×5740 grid: single run DMC (—), average over 3 runs DMC (—), DD with ($\diamond$) and without (– –) the correction to account for back diffusion.

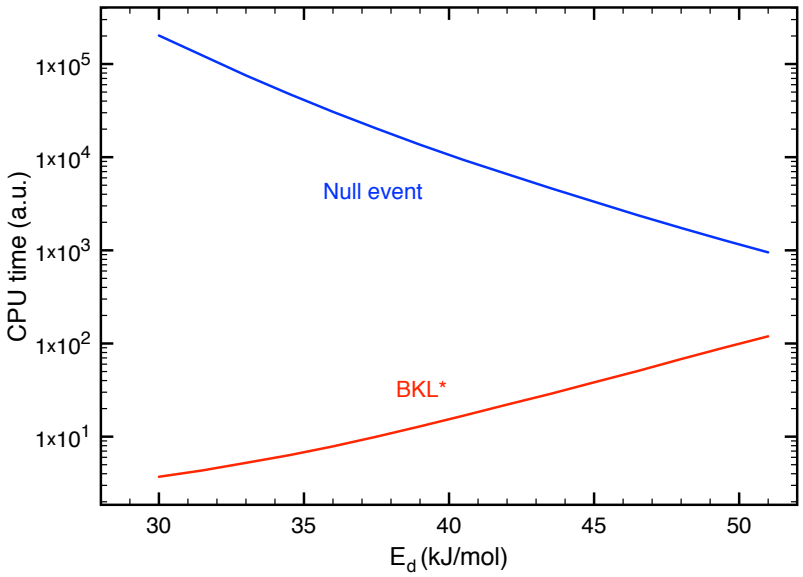

Figure 11. CPU time as a function of the desorption energy on a 2000×2000 grid and $\nu_D = 10^{12}$ s^{-1}, for DMC simulation using the null event (—) and the BKL* (—) algorithms.

be less inadequate, since the difference between the rates of the different processes is smaller (r_2 and τ_D^{-1} become, respectively, 2.0×10^6 and 4.4×10^7 site^{-1}s^{-1} for $E_d = 50$ kJ/mol, the other rates remaining as in table 2). This qualitative indication is confirmed in figure 11, where the CPU time used with the different algorithms is shown. There is a spectacular increase in the performance of the null event DMC scheme as E_d increases, even if the average rates still spread over 6 orders of magnitude for the most favourable case. Inspection of figure 11 and table 3 strongly suggests that a BKL* variant is better suited for DMC surface studies.

4. Conclusions

In this work different stochastic dynamical Monte Carlo (DMC) algorithms to study heterogeneous molecule formation in plasmas and afterglows were implemented, tested, compared with the traditional mesoscopic deterministic description (DD) of surface kinetics, and validated. DMC methods proved to be very powerful tools for this type of investigation. They are exact, easy to implement, run relatively quickly if appropriated chosen and used, handle easily time-dependent probabilities and/or probabilities that depend on the surface configuration, are adaptable to sets of surface reactions with an arbitrary degree of complexity, can be coupled with gas phase chemistry, and bring

new and reliable physical insight. Moreover, they can be extremely useful if linked with atomic scale simulations, specially to model systems of interacting molecules with concentration dependent energy surfaces.

The present study focused on two distinct systems. The first one was NO oxidation on pre-treated pyrex to form NO_2, on a surface that exhibits a *distribution of reactivity* among the chemisorption sites. This system was previously addressed both experimentally and theoretically [27–29], constituting the perfect ground to test and validate the DMC simulations. The n-fold way / Bortz-Kalos-Lebowitz (BKL) [56] dynamical Monte Carlo algorithm proved to be very efficient, coping with elementary processes with rates spanning over several orders of magnitude. The simulations involved a simple but actual *coupling between gas phase and surface chemistries*, as well as elementary *reaction probabilities that depend on time* according to the variation of he gas phase concentrations. The possibility to use a smaller number of sites in the simulation at the expense of averaging over more realisations of the system was established, an approach that can be especially beneficial if several computer cores are available.

The second system studied was oxygen recombination on silica forming O_2. This system is much more challenging due to the presence of surface *reactions involving physisorbed atoms*. These reactions enlarge the range of time-scales associated with the different elementary processes and require the use of significantly large grids to represent the surface, since the fractional coverage of physisorption sites is usually quite low. It was shown that the DMC are feasible using an "hybrid" variation of the BKL algorithm, where no list of empty physisorption sites is kept and "null events" can be selected in the particular case of physisorption. With the new algorithm, the gain in computation time can exceed three orders of magnitude.

From the present investigation it is concluded that an hybrid BKL is most likely the best suited algorithm for DMC simulation of heterogeneous processes. However, there is no universal recipe and a prior analysis of the system is strongly recommended, in order to decide which events shall be treated within the standard BKL formalism and which ones shall not. DMC simulations have further shown the influence of *back diffusion*, associated with the revisit of the same adsorption site by a diffusing atom, and how to include it in the DD. The steady-state properties were not affected by this phenomenon, but the transient time-evolution was. Finally, the role of Langmuir-Hinselwood *recombination involving two physisorbed atoms* was pointed out. Its influence becomes noticeable when the fractional coverage of physisorption sites increases, in compliance with the conclusions from [46, 47].

Besides the development of dynamic Monte Carlo as an instrument to study plasma-surface reactions, the systems analysed here are already quite rich and have a large potential for further research. For instance, the oxygen recombination system can be generalised to account for a distribution of reactivity among different chemisorption sites similar to the one considered for the NO oxidation system, to include physisorption of O_2 molecules and O_3 formation on the wall, or to add either N_2 or CO to the system and study the formation of NO and NO_2 or CO_2 at the wall, respectively. Additional

experimental results are always desirable. Measurements at low wall temperatures and/or relatively high fluxes of atomic oxygen would be extremely valuable, as a way to produce a high coverage of physisorption sites and evince Langmuir-Hinshelwood recombination from these sites.

Acknowledgments

We would like to thank Dr. Dmitry Lopaev and Dr. Bruno Lopez for very fruitful and enlightening discussions. VG was partially supported by Portuguese FCT – Fundação para a Ciência e a Tecnologia, under Projects UID/FIS/50010/2013 and PTDC/FIS-PLA/2135/2012.

References

[1] J. Benedikt, R. Woen, S. L. M. van Mensfoort, V. Perina, and M. C. m. J. Hong, "Plasma chemistry during the deposition of a-C:H films and its influence on film properties," *Diamond Relat. Mater.*, vol. 12, pp. 90–97, 2003.

[2] V. Hody, T. Belmonte, C. D. Pintassilgo, F. Poncin-Epaillard, T. Czerwiec, G. Henrion, Y. Segui, and J. Loureiro, "Modification of hexatriacontane by O_2–N_2 microwave post-discharges," *Plasma Chem. Plasma Process.*, vol. 26, pp. 251–266, 2006.

[3] R. Reuter, K. Rügner, D. Ellerweg, T. de los Arcos, A. von Keudell, and J. Benedikt, "The role of oxygen and surface reactions in the deposition of silicon oxide like films from HMDSO at atmospheric pressure," *9*, pp. 1116–1124, 2012.

[4] F. Zaera, "Mechanisms of surface reactions in thin solid film chemical deposition processes," *Coord. Chem. Rev.*, vol. 257, pp. 3177–3191, 2013.

[5] J. Van Durme, J. Dewulf, C. Leys, and H. Van Langenhove, "Combining non-thermal plasma with heterogeneous catalysis in waste gas treatment: a review," *Appl. Catal. B*, vol. 78, pp. 324–333, 2008.

[6] O. Guaitella, C. Lazzaroni, D. Marinov, and A. Rousseau, "Evidence of atomic adsorption on TiO_2 under plasma exposure and C_2-H_2 surface reactivity," *Appl. Phys. Lett.*, vol. 97, p. 011502, 2010.

[7] T. Ohshima, T. Kondo, N. Kitajima, and M. Sato, "Adsorption and plasma decomposition of gaseous acetaldehyde on fibrous activated carbon.," *IEEE Trans. Ind. Appl.*, vol. 46, pp. 23–28, 2010.

[8] H. Huang, Y. Xu, Q. Feng, and D. Leung, "Low temperature catalytic oxidation of volatile organic compounds: a review," *Catal. Sci. Technol.*, vol. 5, pp. 2649–2669, 2015.

[9] V. Kovalev and A. Kolesnikov, "Experimental and theoretical simulation of heterogeneous catalysis in aerothermochemistry (a review)," *Fluid Dynamics*, vol. 40, pp. 669–693, 2005.

[10] A. Bourdon and A. Bultel, "Numerical simulation of stagnation line nonequilibrium airflows for reentry applications," *J. Thermophys. Heat Trans.*, vol. 22, pp. 168–177, 2008.

[11] J. Marschall and M. MacLean, "Finite-rate surface chemistry model, I: Formulation and reaction system examples," *AIAA Paper 2011-3783*, 2011.

[12] G. A. Curley, L. Gatilova, S. Guilet, S. Bouchoule, G. S. Gogna, N. Sirse, S. Karkari, and J. P. Booth, "Surface loss rates of H and Cl radicals in an inductively coupled plasma etcher derived from time-resolved electron density and optical emission measurements," *J. Vac. Sci. Technol. A*, vol. 28, pp. 360–372, 2010.

[13] M. Sode, T. Schwarz-Selinger, W. Jacob, and H. Kersten, "Surface loss probability of atomic hydrogen for different electrode cover materials investigated in H_2-Ar low-pressure plasmas," *J. Appl. Phys.*, vol. 116, p. 013302, 2014.

[14] B. Rouffet, F. Gaboriau, and J. P. Sarrette, "Pressure dependence of the nitrogen atom recombination probability in late afterglows," *J. Phys. D: Appl. Phys.*, vol. 43, p. 185203, 2010.

[15] G. Oinuma, Y. Inanaga, Y. Tanimura, M. Kuzumoto, Y. Tabata, and K. Watanabe, "A comparative study of the surface recombination of nitrogen atoms on various materials at atmospheric pressure," *J. Phys. D: Appl. Phys.*, vol. 43, p. 255202, 2010.

[16] D. Marinov, O. Guaitella, T. de los Arcos, A. von Keudell, and A. Rousseau, "Adsorption and reactivity of N and O atoms on oxide surfaces," *J. Phys. D: Appl. Phys.*, vol. 47, p. 475204, 2014.

[17] P. F. Kurunczi, J. Guha, and V. M. Donnelly, "Recombination reactions of oxygen atoms on an anodized aluminum plasma reactor wall, studied by a spinnin wall model," *J. Phys. Chem. B*, vol. 109, pp. 20989–20998, 2005.

[18] B. A, G. Cartry, and A. Granier, "Investigation of O-atom kinetics in O_2, CO_2, H_2O and O_2/HMDSO low pressure radiofrequency pulsed plasmas by time-resolved optical emission spectroscopy," *Plasma Sources Sci. Technol.*, vol. 16, pp. 597–605, 2007.

[19] L. Stafford, R. Khare, J. Guha, V. M. Donnelly, J.-S. Poirier, and J. Margot, "Recombination of chlorine atoms on plasma-conditioned stainless steel surfaces in the presence of adsorbed Cl_2," *J. Phys. D: Appl. Phys.*, no. 42, p. 055206, 2009.

[20] B. F. Gordiets and C. M. Ferreira, "Self-consistent modeling of volume and surface processes in air plasma," *AIAA Journal*, vol. 36, pp. 1643–1651, 1998.

[21] M. Castillo, V. Herrero, I. Mendez, and I. Tanarro, "Spectrometric and kinetic study of a modulated glow air discharge," *Plasma Sources Sci. Technol.*, vol. 13, pp. 343–350, 2004.

[22] M. Castillo, I. Mendéz, A. M. Islyaikin, V. J. Herrero, and I. Tanarro, "Low-pressure DC air plasmas. investigation of neutral and ion chemistry," *J. Phys. Chem. A*, vol. 109, pp. 6255–6263, 2005.

[23] K. Kutasi and J. Loureiro, "Role of the wall reactor material on the species density distributions in an N_2–O_2 post-discharge for plasma sterilization," *J. Phys. D: Appl. Phys.*, vol. 40, pp. 5612–5623, 2007.

[24] R. A. B. Zijlmans, S. Welzel, O. Gabriel, G. Yagci, J. H. van Helden, J. Röpcke, D. C. Schram, and R. Engeln, "Experimental study of surface contributions to molecule formation in a recombining N_2/O_2 plasma," *J. Phys. D: Appl. Phys.*, vol. 43, p. 115204, 2010.

[25] D. Marinov, O. Guaitella, A. Rousseau, and Y. Ionikh, "Production of molecules on a surface under plasma exposure: example of NO on pyrex," *J. Phys. D: Appl. Phys.*, vol. 43, p. 115203, 2010.

[26] D. A. Pejaković, J. Marschall, L. Duan, and M. P. Martin, "Nitric oxide production from surface recombination of oxygen and nitrogen atoms," *J. Thermophys. Heat Trans.*, vol. 22, pp. 178–186, 2008.

[27] O. Guaitella, M. Hübner, S. Welzel, D. Marinov, J. Röpcke, and A. Rousseau, "Evidence for surface oxidation on Pyrex of NO into NO_2 by adsorbed O atoms," *Plasma Sources Sci. Technol.*, vol. 19, p. 45026, 2010.

[28] O. Guaitella, M. Hübner, D. Marinov, V. Guerra, C. D. Pintassilgo, S. Welzel, J. Röpcke, and A. Rousseau, "Oxidation of NO into NO_2 by surface adsorbed O atoms," *Contr. Plasma Phys.*, vol. 51, pp. 176–181, 2011.

[29] V. Guerra, D. Marinov, O. Guaitella, and A. Rousseau, "NO oxidation on plasma pretreated Pyrex: the case for a distribution of reactivity of adsorbed O atoms," *J. Phys. D: Appl. Phys.*, vol. 47, p. 224012, 2014.

[30] C. Janssen and B. Tuzson, "Isotope evidence for ozone formation on surfaces," *J. Phys. Chem. A*, vol. 114, pp. 9709–9719, 2010.

[31] D. Marinov, O. Guaitella, J. P. Booth, and A. Rousseau, "Direct observation of ozone formation on SiO_2 surfaces in O_2 discharges," *J. Phys. D: Appl. Phys.*, vol. 46, pp. 032001–1–4, 2013.

[32] W. Choi and M. T. leu, "Kinetics of the heterogeneous reaction $CO+O \rightarrow CO_2$ on inorganic oxide and water ice surfaces: Implications for the martian atmosphere," *Geophys. Res. Lett.*, vol. 24,

pp. 2957–2960, 1997.

[33] V. Kovalev, N. Afonina, and V. Gromov, "Heat transfer modelling to catalytic protection systems of space vehicles entering into martian atmosphere," in *Shock Waves* (Z. Jiang, ed.), pp. 597–602, Springer Berlin Heidelberg, 2005.

[34] A. Bogaerts, M. Eckert, M. Mao, and E. Neyts, "Computer modelling of the plasma chemistry and plasma-based growth mechanisms for nanostructured materials," *J. Phys. D: Appl. Phys.*, vol. 44, p. 174030, 2011.

[35] V. L. Kovalev, A. A. Kroupnov, M. Ju. Pogosbekian, and L. P. Sukhanov, "Simulation of oxygen atom heterogeneous recombination on Al_2O_3 from ab initio approach," *Progress in Flight Physics*, vol. 3, pp. 351–364, 2012.

[36] E. Despiau-Pujo, A. Davydova, G. Cunge, L. Delfour, L. Magaud, and D. B. Graves, "Elementary processes of H_2 plasma-graphene interaction: A combined molecular dynamics and density functional theory study," *J. Appl. Phys.*, vol. 113, p. 114302, 2013.

[37] P. Norman, T. E. Schwartzentruber, H. Leverentz, S. Luo, R. M.-P. neda, Y. Paukku, and D. G. Truhlar, "The structure of silica surfaces exposed to atomic oxygen," *J. Phys. Chem. C*, vol. 117, pp. 9311–9321, 2013.

[38] E. Neyts and A. Bogaerts, "Understanding plasma catalysis through modelling and simulation - a review," *J. Phys. D: Appl. Phys.*, vol. 47, p. 224010, 2014.

[39] M. Rutigliano, P. Gamallo, R. Sayós, S. Orlandini, and M. Cacciatore, "A molecular dynamics simulation of hydrogen atoms collisions on an H-preadsorbed silica surface," *Plasma Sources Sci. Technol.*, vol. 23, p. 045016, 2014.

[40] K. Mizotani, M. Isobe, M. Fukasawa, K. Nagahata, T. Tatsumi, and S. Hamaguchi, "Molecular dynamics simulation of silicon oxidation enhanced by energetic hydrogen ion irradiation," *J. Phys. D: Appl. Phys.*, vol. 48, p. 152002, 2015.

[41] Y. C. Kim and M. Boudart, "Recombination of O, N, and H atoms in silica: Kinetics and mechanism," *Langmuir*, vol. 7, pp. 2999–3005, 1991.

[42] D. A. Stewart, Y. K. Chen, and W. D. Henline, "Effect of nonequilibrium flow chemistry and surface chemistry on surface heating to AFE," *AIAA Paper*, no. 91–1371, 1991.

[43] W. A. Seward and E. J. Jumper, "Model for oxygen recombination on silicon-dioxide surfaces," *J. Thermophys. Heat Trans.*, vol. 5, pp. 284–291, 1991.

[44] G. Cartry, L. Magne, and G. Cernogora, "Atomic oxygen recombination on fused silica: Modelling and comparison to low-temperature experiments (300 k)," *J. Phys. D: Appl. Phys.*, vol. 33, pp. 1303–1314, 2000.

[45] V. Guerra, "Analytical model of heterogeneous atomic recombination on silicalike surfaces," *IEEE Trans. Plasma Sci.*, vol. 35, pp. 1397–1412, 2007.

[46] D. V. Lopaev, E. M. Malykhin, and S. M. Zyryanov, "Surface recombination of oxygen atoms in O_2 plasma at increased pressure: I. The recombination probability and phenomenological model of surface processes," *J. Phys. D: Appl. Phys.*, vol. 44, pp. 015201–1–12, 2011.

[47] D. V. Lopaev, E. M. Malykhin, and S. M. Zyryanov, "Surface recombination of oxygen atoms in O_2 plasma at increased pressure: II. Vibrational temperature and surface production of ozone," *J. Phys. D: Appl. Phys.*, vol. 44, pp. 015202–1–16, 2011.

[48] K. A. Fichthorn and W. H. Weinberg, "Theoretical foundations of dynamical monte carlo simulations," *J. Chem. Phys.*, vol. 95, pp. 1090–1096, 1991.

[49] J. S. Reese, S. Raimondeau, and D. G. Vlachos, "Monte carlo algorithms for complex surface reaction mechanisms: Efficiency and accuracy," *J. Comput. Phys.*, vol. 173, pp. 302–321, 2001.

[50] V. Guerra and J. Loureiro, "Dynamical monte carlo simulation of surface atomic recombination," *Plasma Sources Sci. Technol.*, vol. 13, pp. 85–94, 2004.

[51] V. Rai, H. Pitsch, and A. Novikov, "Efficient dynamic monte carlo algorithm for time-dependent catalytic surface chemistry," *Phys. Rev. E*, vol. 74, pp. 046707–1–9, 2006.

[52] V. L. Kovalev, V. Yu. Sazonenko, and A. N. Yakunchikov, "Dynamic Monte Carlo simulation of surface recombination," *Mosc. Univ. Mech. Bull.*, vol. 62, pp. 53–58, 2007.

[53] H. M. Cuppen, L. J. Karssemeijer, and T. Lamberts, "The kinetic monte carlo method as a way to solve the master equation for interstellar grain chemistry," *Chem. Rev.*, vol. 113, pp. 8840–8871, 2013.

[54] D. T. Gillespie, "A general method for numerically simulating the stochastic time evolution of coupled chemical reactions," *J. Comput. Phys.*, vol. 22, pp. 403–434, 1976.

[55] D. T. Gillespie, "Exact stochastic simulation of coupled chemical reactions," *J. Phys. Chem.*, vol. 81, pp. 2340–2361, 1977.

[56] A. B. Bortz, M. H. Kalos, and J. L. Lebowitz, "a new algorithm for Monte Carlo simulation of king spin Systems," *J. Comput. Phys.*, vol. 17, pp. 10–18, 1975.

[57] J. C. Graves and J. W. Linnett, "Recombination of atoms at surfaces, part 6 - recombination of oxygen atoms on silica from 20^o C to 600 ^{o} C," *Trans. Faraday Soc.*, vol. 55, pp. 1355–1361, 1959.

[58] D. Marinov, V. Guerra, O. Guaitella, J. P. Booth, and A. Rousseau, "Ozone kinetics in low-pressure discharges: vibrationally excited ozone and molecule formation on surfaces," *Plasma Sources Sci. Technol.*, vol. 22, p. 055018, 2013.

[59] H. Ibach, W. Erley, and H. Wagner, "The preexponential factor in desorption – CO on Ni(111)," *Surf. Sci.*, vol. 92, pp. 29–42, 1980.

[60] K. Christmann, *Introduction to Surface Physical Chemistry.* Topics in Physical Chemistry, Berlin: Springer-Verlag, 1991.

[61] P. Macko, P. Veis, and G. Cernogora, "Study of oxygen atom recombination on a pyrex surface at different wall temperatures by means of time-resolved actinometry in a double pulse discharge technique," *Plasma Sources Sci. Technol.*, vol. 13, pp. 251–262, 2004.

[62] S. Cazaux, P. Caselli, A. G. G. M. T. abd J. Le Bourlot, and M. Walmsley, "Molecular hydrogen formation on grain surfaces," *J. Phys.: Conf. Series*, vol. 6, pp. 155–160, 2005.